Experimental Study of the Formation of CO during Ethanol Pyrolysis and Dry Reforming with CO_2

Olivier Mathieu*, Claire M. Grégoire, Maryam Khan-Ghauri, Sean P. Cooper, Eric L. Petersen

J. Mike Walker '66 Department of Mechanical Engineering, Texas A&M University, College Station, Texas 77845, United States

*Corresponding author: olivier.mathieu@tamu.edu

Highlights:

- Dry reforming of ethanol with CO_2 was studied in a shock tube for the first time
- CO time-history profiles were recorded using a laser absorption diagnostic
- Modern detailed kinetics models cannot replicate the experimental results

Abstract:

To use piston engines and their pressure and temperature histories as a chemical rector to produce valuable chemicals, accurate chemical kinetics models are necessary so the engine parameters and mixtures can be designed. Using piston engines in such a way could lead to the production of target chemicals with net-negative CO_2 emissions. This benefit is especially true for ethanol, a very common biofuel. To validate models, the dry reforming of ethanol and CO_2 was investigated experimentally in a shock tube (50/50 ethanol/CO_2 in 99.75% dilution) by following the formation of CO with a laser absorption setup. The effect of the presence of CO_2 in the mixture was also investigated by comparing the results of the 50/50 ethanol/CO_2 mixture with those from the pyrolysis of ethanol (without CO_2) at various concentrations (99.75 and 98% dilution). The 98% dilution results compare extremely well with results from the literature, whereas the other conditions had never been investigated prior. The experimental data were compared to modern detailed kinetics mechanisms, and the experimental CO profiles were poorly predicted overall. Recent literature developments on ethanol pyrolysis were incorporated into the models, and the predictions were improved in some cases and conditions, although further improvements are still necessary. A numerical analysis (rate of production and sensitivity) was performed for the most accurate modified model to highlight the most important reactions involved in the formation of CO under our conditions.

Keywords: ethanol, shock tube, pyrolysis, reforming, CO formation

1. Introduction:

During the past 120 years, piston engines have been instrumental in the development and growth of the road transportation sector. The popularization of automotives powered by piston engines in the first half of the past century led to a profound transformation of our societies, allowing freedom of movement for billions of people to a level that would have been hard to imagine only a few decades before. However, this large usage of vehicles powered by piston engines led to problems associated with their emissions. First, pollutant emissions due to combustion (NOx, SOx, unburned hydrocarbons, soot) have rapidly been found detrimental to the

health of the people and the environment. Technological advancements and gradually stricter policies have been successfully implemented in developed countries to greatly limit these emissions to levels that are now acceptable. The other important issue with piston engines is that they have essentially operated on fossil fuels, which also lead to the increase in the atmospheric CO_2 concentration and global warming. As part of the solution to mitigate this issue, biofuels such as ethanol have been added to petroleum-based fuels. Today, there are large structures dedicated to ethanol production and it is contained in high concentration (up to 20%) in U.S. gasoline and can even reach 85% in Europe (E85). In some countries like Brazil, engines are running on pure ethanol after only minor modifications [1].

Nowadays, with growing concerns about global warming and as battery technology developed, the road transportation sector is slowly transitioning toward electric vehicles. To still take advantage of the maturity, durability, and flexibility of the piston engine in the future, a possible application would be to use them as chemical reactors to efficiently produce valuable chemicals [2]. As explained in the literature [2,3], high pressures and temperatures can be generated in a short time, at the millisecond level, during the compression stroke, and the fast temperature quench of the expansion stroke can allow for the preservation of a target species under a nonequilibrium state, where optimal yield and efficiency are reached. According to Ashok et al. [2], these features are unmatched by any commercial reactor used by the chemical industry. Several chemicals can be targeted depending on the fuel, engine parameters (speed, compression ratio), and conditions (reforming, partial oxidation, or pyrolysis). Among these chemicals, one can mention syngas (a mixture of CO and H_2), C_2H_2, C_2H_4, CH_3OH, or CH_2O. Those chemicals can be used to produce energy, for chemical energy storage, or employed directly in many industries [2,3], notably for syngas [4].

To take advantage of the existing infrastructures for ethanol production and to produce chemicals with a true net-negative CO_2 production, one could use piston engines to produce these chemicals via ethanol in a dry-reforming process (ethanol and CO_2 as reactants, possibly with air, the engine being motored using electricity potentially coming from excess production from renewable sources (solar, wind)). Since the nature and concentration of the chemicals produced depend on the mixture composition (CO_2 proportion, equivalence ratio (ϕ)) and engine parameters (compression ratio and engine speed, defining pressure and temperature histories and residence time, respectively), an accurate kinetics model is necessary to efficiently design the process. While ethanol combustion kinetics have been extensively studied both experimentally [5-17] and numerically [18-24], recent studies show that models could still be improved [25-28]. In addition, it is worth mentioning that the models have not been validated for engine-based energy storage and reforming processes. Thus, there is a need for fundamental research in this area, and the aim of the present study was to assess the accuracy of modern detailed kinetics mechanisms against new CO measurements obtained from the high-temperature reactions between ethanol and CO_2 in a shock tube (at reforming conditions). The formation of CO from ethanol pyrolysis was also investigated herein as a baseline. First in this paper is a description of the shock tube and the laser-absorption diagnostic used to measure the formation of CO behind reflected shock waves. The experimental results are then presented and compared to detailed kinetics models. A chemical analysis is then performed to understand the discrepancies between the models and the data before concluding.

2. Experimental procedure

Experiments were conducted in a stainless-steel, single-diaphragm (polycarbonate, 0.25-mm thickness) shock tube which has been described in previous studies [29]. Briefly, the shock tube has a driver section of 7.62-cm i.d. and 3.25 m long, and a 16.2-cm i.d. and 7.88 m long driven section. Piezoelectric pressure transducers with a well-known spacing between them, located along the driven section, are used to extrapolate the incident shock-wave velocity at the endwall location. This extrapolated velocity was used to determine the temperature (T_5) and pressure (P_5) behind the reflected shock wave using the one-dimensional (1-D) normal

shock equations. The uncertainty in T_5 is within 0.8% (10-15 K). The driven section was vacuumed down to 2 × 10^{-5} Torr or less before each experiment using a turbomolecular pump.

A tunable quantum cascade laser was used to produce light near 4.8 μm to monitor the P(20) line of the $1 \leftarrow 0$ band for the CO time-history measurements. Before each experiment, the CO wavelength is centered at 2059.91 cm^{-1} to the peak of the transition P(20) line with the following conditions for the temperature and current controllers of the laser: 30°C and 195.90 ± 0.05 mA, respectively. The maximum absorption strength is verified with a removable reference cell containing a mixture of ~10% CO/90% Ar at low pressure, allowing for fine tuning. During the combustion processes, no interaction is expected with CO_2 and H_2O at this wavelength [30]. The optical arrangement splits the beam into two components: the time-resolved incident intensity (I_0) and the time-resolved transmitted intensity (I_t). These intensities are processed in conjunction with the Beer-Lambert law to find the CO time histories. The Beer-Lambert relation is defined as

$$I_t/I_0 = exp(-k_\nu PL) \tag{1}$$

where k_ν is the absorption coefficient ($cm^{-1}atm^{-1}$), P is the partial pressure of CO (atm), and L is the path length (16.2 cm, corresponding to the shock-tube inner diameter). As the fuel concentration effect was investigated herein, separate experiments were conducted to characterize k_ν at each condition and infer broadening effects from the major collision partners, the perturbing species He and Ar. This characterization was carried out by measuring a known amount of CO in corresponding He/Ar mixtures over a wide range of temperature (1200 - 2700 K) and around atmospheric pressure. The results are presented in Fig. 1, along with the best fit of the data which yielded the temperature dependency relation of the absorption coefficient.

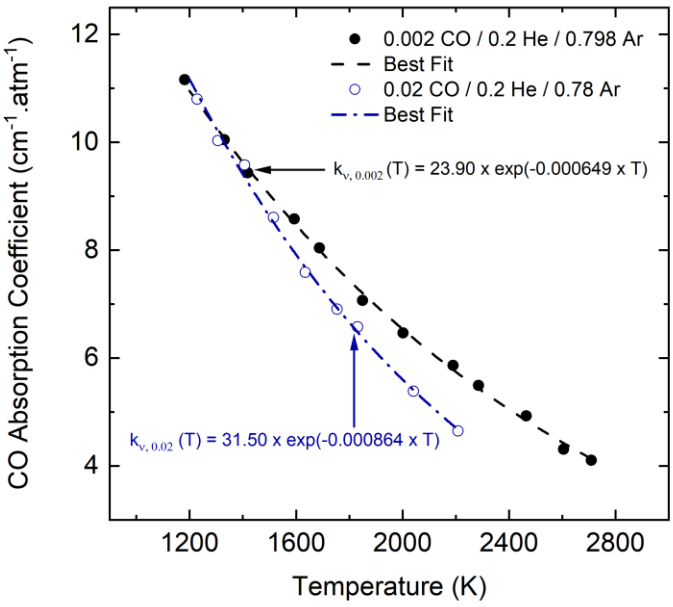

Figure 1: Spectral absorption coefficients of 2000 ppm CO in 0.2/0.798 He/Ar, and 20,000 ppm CO in 0.2/0.78 He/Ar. Dashed and dashed dot lines present the best fit used to calculate $k_{\nu,0.002}$ and $k_{\nu,0.02}$, respectively.

Mixtures containing 2000 ppm (0.2 He/0.798 Ar) and 20,000 ppm of CO (0.2 He/0.78 Ar) were used as an input in the Beer-Lambert law, in conjunction with the measured I_0 and I_t intensities to determine $k_{\nu,0.002}$ and $k_{\nu,0.02}$, respectively. These two absorption coefficients are described with the following temperature-dependent equations with a goodness-of-fit R^2 value of 0.998 for both calibrations:

$$k_{v,0.002} = 23.90\, e^{-0.000649\,T} \quad (2)$$

$$k_{v,0.02} = 31.50\, e^{-0.000864\,T} \quad (3)$$

While the calibration for $k_{v,0.02}$ fits perfectly our 98% dilution, $k_{v,0.002}$ was validated for the 99.75% dilution.

During the experiments, the change in T_5 with time due to the mixtures' reactivity was calculated using the NUIGMech1.1 model [31]. This change in temperature was accounted for in the post processing of the data by utilizing a time-varying k_v. The computed change in temperature over the course of an experiment varies from below 5 K, for the lowest temperature investigated with Mix 3 (see Table 1), and 175 K, for the highest temperature with Mix 1. This leads to a minor reduction in the final CO mole fraction, typically 5% or less [32]. More details on this procedure are available in Alturafi et al. [33], and the estimated uncertainty of the CO measurements is about 3.8 %, as detailed in our previous work [32,34].

The mixtures investigated were prepared manometrically (partial pressure method) in a stainless-steel mixing tank. Ethanol (Sigma-Aldrich, ≥99.5% purity) was introduced via a vial connected to the manifold after being degassed at least three times. Two MKS Baratron capacitance manometers (0–10 Torr and 0–1000 Torr ranges) were used to prepare the mixtures. All gases were high purity (CO_2: 99.99%, Ar and He: 99.999%, Praxair). The mixtures investigated and conditions behind reflected shock waves covered during this study are visible in Table 1. Dilute mixtures were preferred over "real", undilute, mixtures as the high dilution level strongly mitigates the change in temperature and pressure from the reactivity. Thus, the present results are driven by the kinetics of the chemistry and not by the energy release and gas dynamic effects associated with the very energetic undilute mixtures, allowing us to observed important features in the CO profiles (such as the rate of CO formation), which could not be observed otherwise. Note that the 20% He addition to the mixture was necessary to expedite the vibrational relaxation process, as detailed in Mathieu et al. [32].

Table 1: Mixture compositions and experimental conditions investigated.

Mix #	X_{C2H5OH}	X_{CO2}	X_{He}	X_{Ar}	Temperature (K)	Pressure (atm)
1	0.02	0	0.2	0.78	1229 – 1789	1.11 – 1.33
2	0.0025	0	0.2	0.7975	1259 – 1587	1.27 – 1.38
3	0.00125	0.00125	0.2	0.7975	1287 – 1596	1.27 – 1.36

3. Detailed kinetics model selection

Experimental results obtained during this study were compared with detailed kinetics models from the literature. While many models dedicated to - or containing - ethanol were published over the past decade [8,15,19,22,35,36], a former study from our group [26] showed that most models were not suitable to predict laser absorption profiles using a similar method but with H_2O as a target species. The models that were not found adequate [8,19,35] are thus discarded, and only the following models were used in the present study: the most recent CRECK model [22] and the most recent model from the NUIG group [37]. Lastly, the model from Zhang et al. [38] (Polymech2.1), which was developed specifically for the purpose of the present study (i.e., for fuel-rich polygeneration and energy storage processes), was also used. This model was extensively validated against plug-flow reactors, shock tubes, rapid compression machines, and flame data. Chemkin pro was used for the computations using the "Closed homogeneous reactor" module with the "Constant volume and solve energy equations" assumption.

4. Experimental results and model comparison

4.1. Ethanol pyrolysis

The CO profiles obtained during ethanol pyrolysis are visible in Fig. 2 (a) for the 2% ethanol mixture (Mix 1) and Fig. 2 (b) for the 0.25% ethanol mixture (Mix 2). In both cases, the appearance of CO starts right from the beginning of the experiment, and its rate of formation is strongly dependent on temperature. For the lowest temperatures investigated, the CO mole fraction increases slowly and never reaches equilibrium within the time-frame of the experiment. As the temperature increases, a plateau for the CO mole fraction is reached, which is particularly visible for the highest temperatures investigated. Note that the timing at which this plateau is reached is also temperature dependent. Similar profiles are observed for the two mixtures, but Mix 1, with its higher ethanol concentration, produces about ten times more CO than Mix 2 at the plateau value of the highest temperatures investigated. It is worth mentioning that the plateau observed for the high-temperature experiments in Fig. 2 does not correspond to the actual chemical equilibrium amount of CO. More details are provided with the model comparison below.

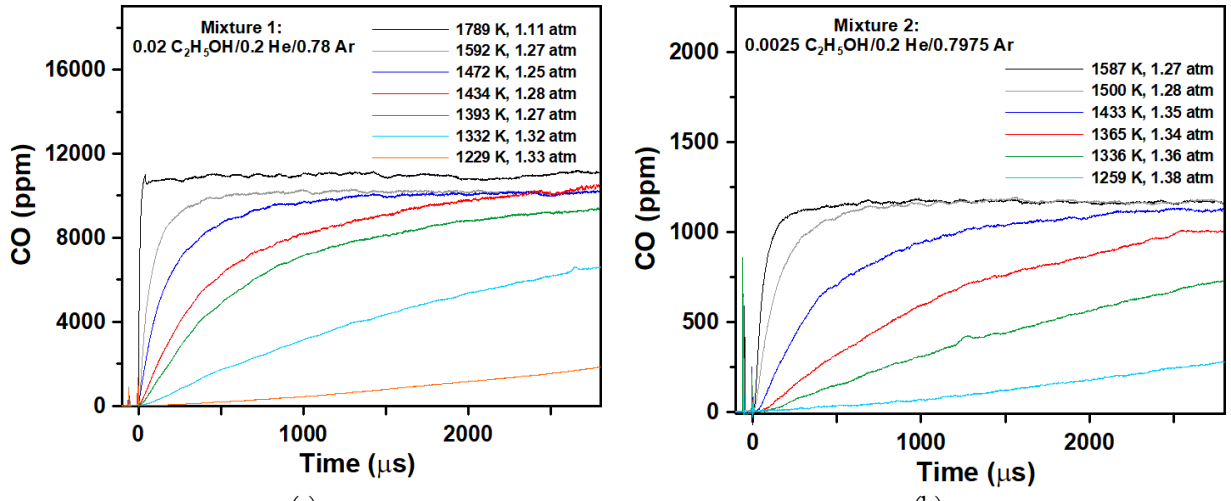

(a) (b)

Figure 2: Time-evolution of the CO profile with temperature during the pyrolysis of ethanol for (a) a mixture of 2% ethanol in 20%He/78% Ar, and (b) a mixture of 0.25% ethanol in 20% He and 79.75% Ar.

For the comparison with the models, only a couple representative experiments for each mixture are presented herein. However, all CO profiles not presented in the paper are compared to the models and are available in Supplementary Material. For Mix 1, profiles on the low and high end of the range of temperatures investigated were used in Fig. 3, 1332 K (a) and 1592 K (b). As can be seen, the models predict the profile at 1332 K with good accuracy overall, with the final value of CO at the end of the test time better captured by the NUIG model and the early formation of CO better predicted by the CRECK model. On the other hand, large discrepancies can be observed between the models for the high-temperature experiment at 1592 K. A 20% difference can be observed between the NUIG (over-estimation) and PolyMech2.1 (under-estimation) models and the data whereas the CRECK model offers accurate predictions concerning the shape, timing, and concentration of the CO profile. Note that at this concentration level of ethanol, the temperature is predicted to decrease by about 115 K according to the models.

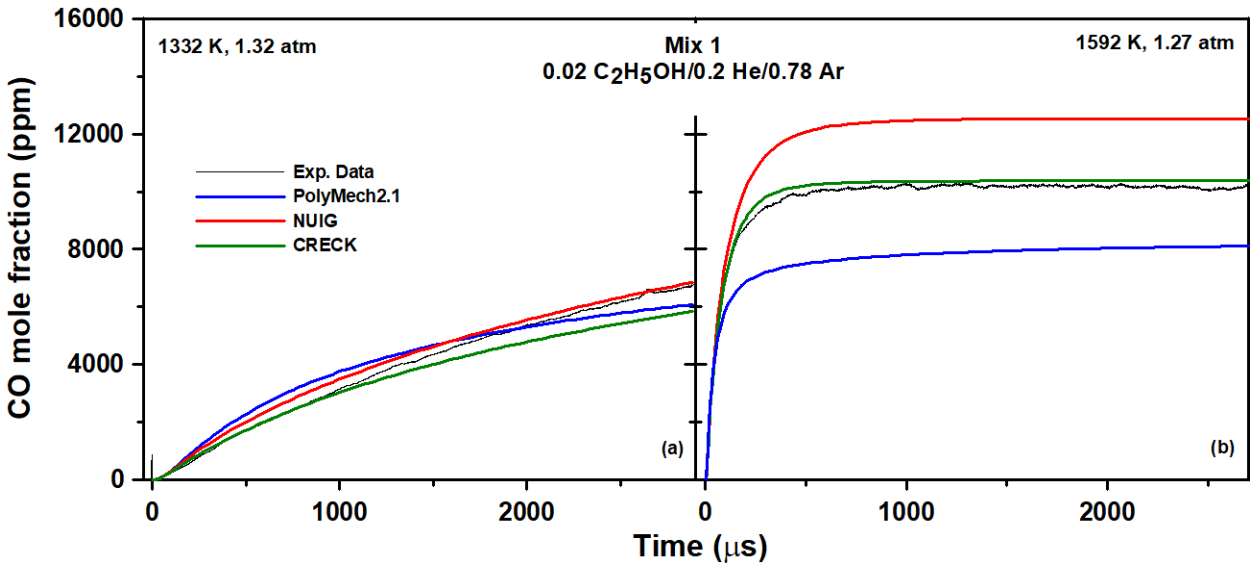

Figure 3: Comparison between selected CO profiles obtained for the pyrolysis of a 2% ethanol mixture in inert gases (Mix 1) and predictions from detailed kinetics models from the literature.

For Mix 2, shown in Fig. 4, the very high level of dilution (99.75%) induces a very small change in temperature over the course of the experiment (models predict a temperature drop less than 25 K at 1587 K). Thus, the predictions from the models are more purely driven by the kinetics of the reactions selected within each model than by any large change in temperature during the time-frame of the experiment. As can be seen, predictions on the low-temperature side, 1365 K (Fig. 4 (a)), are very accurate for the CRECK model, whereas the NUIG model correctly predicts the shape but still over-predicts the CO level by about 20% at the end of the observation time. PolyMech2.1 presents higher accuracy concerning the final level of CO in this particular case, but the predicted shape of the CO profile is different from the experimental one. At high temperature, 1587 K (Fig. 4 (b)), the shape and rate of CO formation are well predicted by all models considered herein. However, notable discrepancies are observed for the equilibrium CO level: over-estimation of the CO level by about 10% and 30% for the CRECK and NUIG models, respectively, and under-prediction by about 15% for the PolyMech2.1 mechanism. As mentioned earlier, the plateau observed experimentally for the highest temperatures does not correspond to the CO level at chemical equilibrium. For instance, taking Mix 2 as an example, the predictions at 1600 K and 1.3 atm show that the equilibrium value for CO is 2481.6 ppm for the PolyMech2.1 model, 2481.4 ppm for CRECK, and 2481.5 ppm for NUIG. This equilibrium level is reached at much later times, between 1 and 2 minutes according to the computation. This common result indicates that the thermochemistry is similar for all models and that the experimental results presented herein are mostly driven by the chemical kinetics, making them powerful tools to assess the detailed kinetics models within the limited timeframe of our experiments.

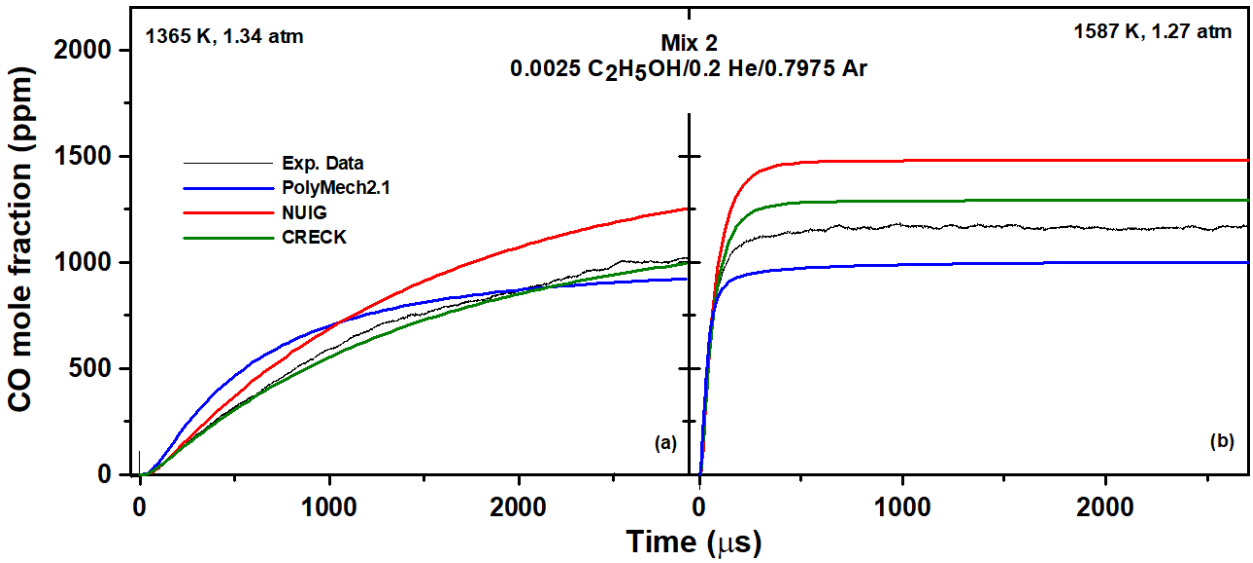

Figure 4: Comparison between selected CO profiles obtained for the pyrolysis of a 0.25% ethanol mixture in inert gases (Mix 2) and predictions from detailed kinetics models from the literature.

4.2. Ethanol/CO_2 pyrolysis

For the mixture with CO_2, Fig. 5, the shape of the profiles and temperature behavior are similar to what was observed for the pyrolysis mixtures in Fig. 1. The mole fraction of CO at the plateau for the highest temperature investigated, 1596 K, comparable to the one in Fig. 2 (b) (1587 K), shows that Mix 3 produces about 62% of the CO measured in Mix 2, for which the ethanol mole fraction is two times higher. This proportionally larger formation of CO from ethanol indicates a conversion of CO_2 into CO during the experiments, as detailed later. Note that the small spikes in the signal at 300 μs/1451 K and 1450 μs/1510 K are not related to CO formation, but most are likely due to very small diaphragm fragments from previous experiments briefly obstructing the laser path despite the frequent cleaning of the apparatus.

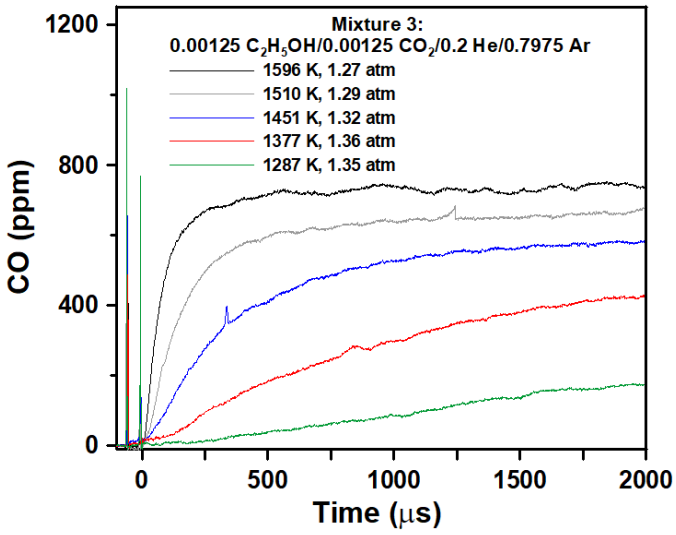

Figure 5: Time evolution of the CO profile with temperature during the pyrolysis of a 50/50 ethanol/CO_2 mixture in 20%He/79.75% Ar.

The comparison between the data and the models for Mix 3 is visible in Fig. 6. For this case, three profiles were selected to illustrate various behaviors from the models: 1377 K (a), 1510 K (b), and 1596 K (c). At the lowest temperature, results are similar to the low-temperature case in Fig. 4: accurate prediction of the CRECK model, prediction of the shape but over-predictions of the CO level by NUIG, and good prediction of the final CO level but poor prediction of the profile's shape by the PolyMech 2.1 model. At 1510 K, Fig. 6(b), the plateau is reached by the data and the models. The CO concentration at the plateau is accurately predicted by the CRECK model whereas the PolyMech2.1 model under-predict this value by about 30% and the NUIG model over-predicts it by about 15-20%. On the other hand, focusing on the first 300 μs, one can see that the initial formation (timing and slope) of the CO profile is well characterized by the NUIG and PolyMech2.1 mechanisms, whereas the CRECK model is slightly under-reactive. Interestingly, for the highest temperature investigated, 1596 K (Fig. 6 (c)), the steady increase in the CO concentration at the plateau when CO_2 is present is not fully captured by the model. As a result, the NUIG model is now very close to the experimental data, while the CRECK model under-predicts the CO level by about 10-15%. A larger discrepancy was observed for the PolyMech2.1 model, with an under-prediction of the CO level by about 40%.

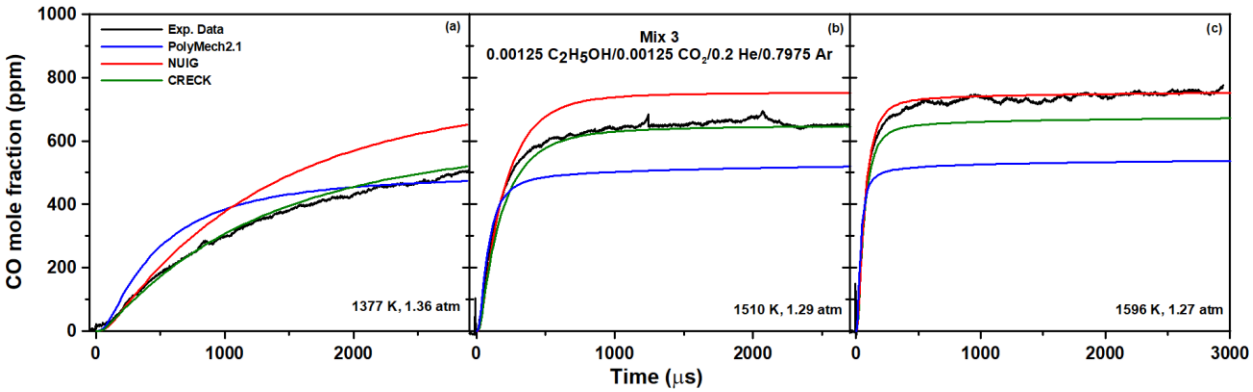

Figure 6: Comparison between selected CO profiles obtained for the pyrolysis of a 0.125% ethanol/0.125% CO_2 mixture in inert gases (Mix 3) and predictions from detailed kinetics models from the literature at (a) 1377 K, (b) 1510 K, and (c) 1596 K.

5. Discussion

As seen above, predictions for CO time histories for ethanol pyrolysis, in the presence or not of CO_2, could be improved. Interestingly, Choudhary et al. [27,28] recently measured CO formation during ethanol pyrolysis in conditions very close to the conditions covered herein for Mix 1. In their study, the AramcoMech3.0 model compared very well with their data, whereas the latest NUIG model used in the present study shows large over-predictions at high temperatures, Fig. 3(b). Data from the present study and from the study of Choudhary et al. were compared for similar temperatures (Fig. 7) and, as shown, the data are extremely repeatable between the two groups. In more detail, for similar temperature and pressure (Fig. 7(a)), the two sets of data are identical at around 1330 K. At a higher temperature of 1440±6 K (Fig. 7(b)), the data are again on top of each other for the most part, and a small discrepancy is observed past 700 μs. This discrepancy can be due to the pressure

difference between the studies or to run-to-run variability. It is difficult to fully judge the difference between the two datasets for the final CO concentration as the test time is different (more than double for the present study). At higher temperatures (Fig. 7 (c)), the temperatures between the two studies are different, but one can see that the reactivity (characterized by the time at which the plateau is reached, and/or slope of the CO formation phase) follows a logical order between the two studies. Moreover, the CO level at the plateau is similar for all experiments (an error bar corresponding to the 3.8% uncertainty in our measurements was placed on the highest-temperature data for reference). This comparison between the results of the two studies indicates that discrepancies between the model and the data observed in Figs. 3, 4 and 6 are likely coming from the model, and that the good agreement between the Choudhary study and the predictions of the AramcoMech3.0 model is due to the fact that the experimental data were not conducted for long enough times (to actually observe the disagreement with the model) and/or at high enough temperatures so that the plateau is fully reached within the test time of the Choudhary et al. study.

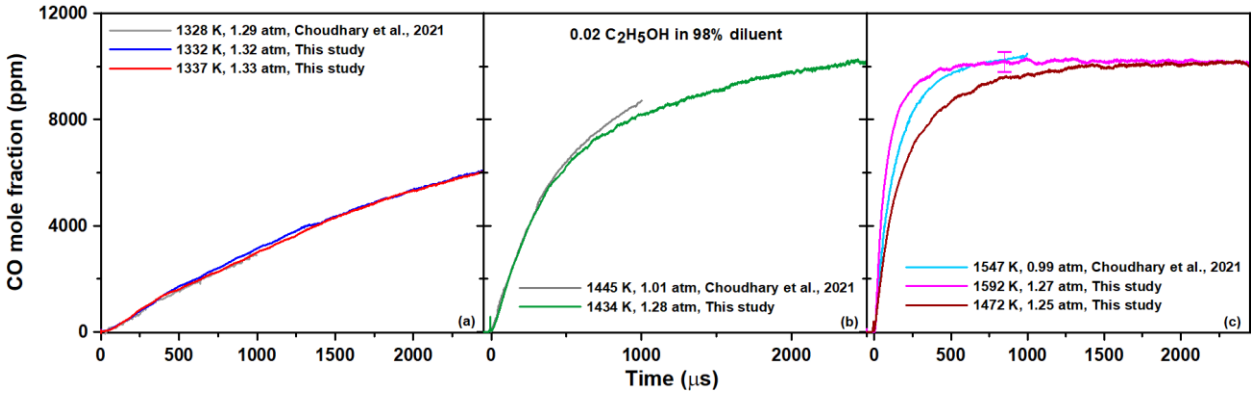

Figure 7: Comparison between the experimental data of the present study and the data from Choudhary et al. [27,28].

Since the models used herein are not capable of accurately predicting our data, the rate coefficients determined in the study of Choudhary et al. were implemented into these models in an attempt to improve the predictions. Results (visible in Sup. Mat) show that the implementation of the updated rate coefficients for ethanol chemistry from Choudhary et al. leads to a large degradation of the predictions from the Polymech2.1 model. Concerning the other models considered, the implementation of the rate coefficients from Choudhary et al. consistently improved the predictions for the NUIG model (except for the highest temperature for Mix 3), whereas a more contrasted effect, depending on the mixture and temperature, was observed for the CRECK model. The modified model (NUIG+Choudhary), while still insufficient to correctly model the data over the entire range of conditions investigated, is then used herein to analyze the results and to provide guidance to further improve the predictions. Note that the rate coefficient for the reaction $C_2H_5OH \leftrightarrows C_2H_4 + H_2O$ determined by Pinzón et al. [39] in the same shock tube and under similar conditions as the present study was also tried. However, its implementation did not provide any improvement over the rates proposed in Choudhary et al. or even slightly deteriorated the predictions in some cases.

The modified model was used to conduct a sensitivity analysis on CO with the dedicated Chemkin tool [40] (top ten reactions only using the peak sensitivity) for Mix 2 and 3 (same dilution level, with or without CO_2, respectively), on the low- (1370 K) and high-temperature (1590 K) side of the range investigated. Results for the normalized coefficients (taken at the peak sensitivity value) are visible in Fig. 8 and show that the most

promoting and inhibiting reactions are the same for the two mixtures and temperatures considered (the reaction number correspond to the reaction number in the modified NUIG mechanism): $C_2H_5OH \leftrightarrows CH_3 + CH_2OH$ (R519, promoting) and $C_2H_5OH \leftrightarrows C_2H_4 + H_2O$ (R518, inhibiting). R518 is inhibiting as this reaction pathway produces two stable molecules which do not lead to CO formation by themselves. On the other hand, R519 produces two reactive molecules, including CH_2OH which will then lead to CO via R202, R182, -R179, and R192 (all sensitive, promoting reactions for both mixtures in Fig. 8). Note that R518 and R519 are both reactions that have been determined in the study from Choudhary et al. [27,28].

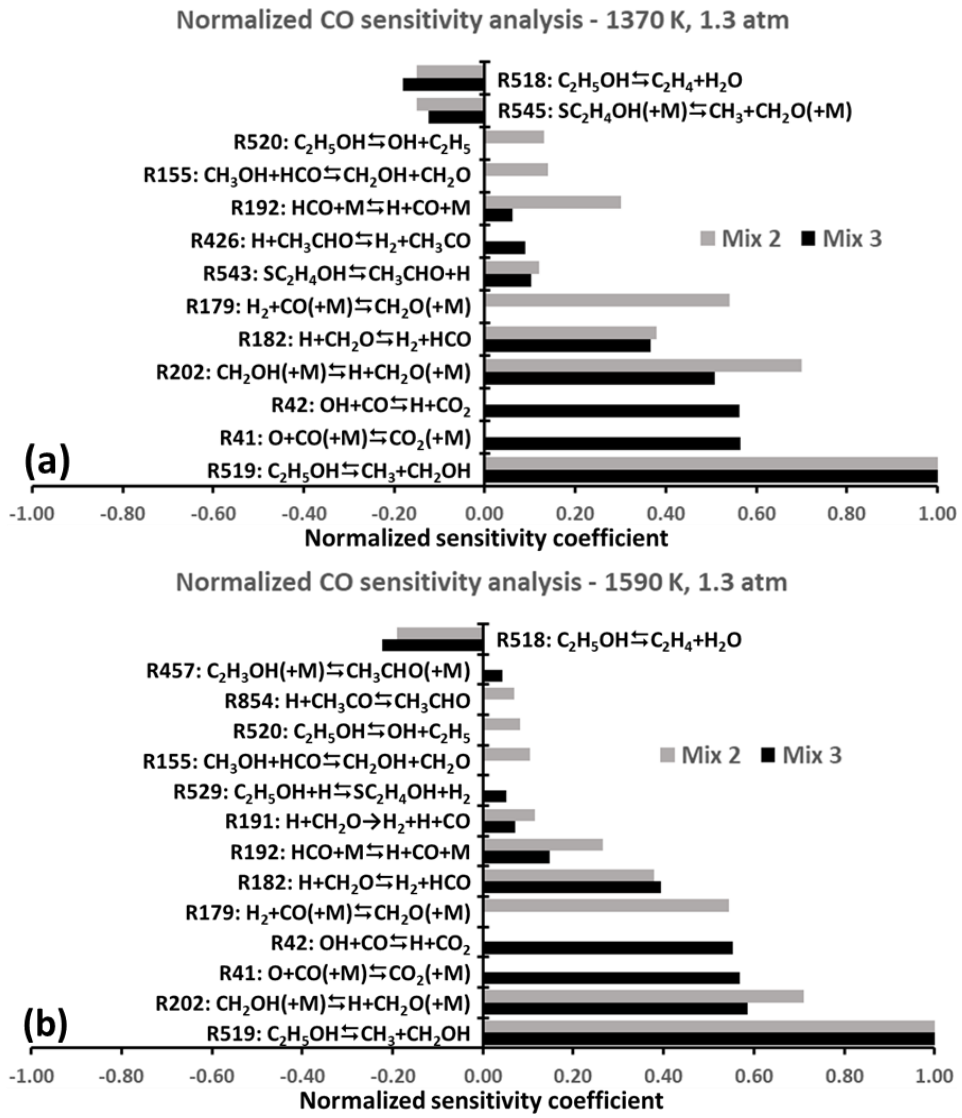

Figure 8: Normalized sensitivity analysis for CO for mixtures 2 and 3 at (a) 1370 K and (b) 1590 K, 1.3 atm.

With presence of CO_2 in Mix 3, two sensitive reactions appear (both in reverse), R41 ($O + CO(+M) \leftrightarrows CO_2(+M)$) and R42 ($OH + CO \leftrightarrows CO_2 + H$). These two reactions each form CO from CO_2, either by thermal dissociation (R41) or by reacting with H radicals coming from ethanol pyrolysis. Note that despite the relatively high sensitivity of these two reactions, a rate of production analysis shows that the production of CO from

CO_2 is actually very small under the conditions of the present study but grows in importance as the temperature increases. This increase in importance translates experimentally to a higher concentration of CO as the temperature increases for Mix 3 (Fig. 5), which is not fully captured by the models (Fig. 6). Models are also presenting poorer performances as the temperature increases for the experiments with Mix 3. According to this analysis, the two main reactions producing CO are, by far, R192 (HCO + M ⇆ H + CO + M) and R444 ($CH_3CO(+M)$ ⇆ $CO+CH_3(+M)$. While R192 is relatively well-known (see discussion in [32]), it is worth mentioning that the rate coefficient varies widely, by a factor of between 20 and 60 in the conditions of the study, between the one selected in the NUIG model (coming from the theoretical work of Senosiain et al. [41]) and the one determined experimentally by Faravelli et al. [42], for example. A careful, modern, study of R444 could possibly improve the predictions for ethanol pyrolysis.

6. Conclusion

The formation of CO was followed using a laser absorption diagnostic from ethanol pyrolysis in diluents (baseline, 99.25 and 98 % dilution) and in the presence of a large proportion of CO_2 (50% ethanol/50% CO_2, 99.25% dilution) to assess the validity of modern detailed kinetics mechanisms. It was found that these modern mechanisms cannot accurately predict ethanol pyrolysis, with and without the presence of CO_2. The recent rate coefficients for ethanol pyrolysis reactions obtained by Choudhary et al. were implemented in these models, and while noticeable improvements were observed in most cases, predictions could still be greatly improved. A numerical analysis was conducted using the modified NUIG model, and the analysis showed that the most sensitive reactions are common between the two types of mixtures. In the presence of CO_2, additional reaction pathways for CO appear, with one pathway involving H radicals formed during the pyrolysis of ethanol. This study shows that the formation of CO appears at relatively low temperatures due to the high reactivity of ethanol, although an increasing amount of CO was observed experimentally as the temperature increases in presence of CO_2, a behavior that was not captured by the models. It can be concluded that more work is necessary to fully understand ethanol pyrolysis and its interactions with CO_2. Future work should also involve higher pressures, more representative of engine conditions.

7. Acknowledgments

The authors would like to thank the National Science Foundation for the financial support of this study (award # 2037795). Additional support came from the TEES Turbomachinery Laboratory through a Ralph-James Fellowship for CMG.

8. References

[1] Delgado RCOB, Araujo AS, Fernandes Jr VJ. Properties of brazilian gasoline mixed with hydrated ethanol for flex-fuel technology, Fuel Process. Technol., 2007;88:365–368. doi:10.1016/j.fuproc.2006.10.010

[2] Ashok A, Katebah MA, Linke P, Kumar D, Arora D, Fischer K, Jacobs T, Al-Rawashdeh M. Review of piston reactors for the production of chemicals. Reviews in Chemical Engineering, 2021: 000010151520200116. https://doi.org/10.1515/revce-2020-0116

[3] Atakan B, Kaiser SA, Herzler J, Porras S, Banke K, Deutschmann O, Kasper T, Fikri M, Schießl R, Schroder D, Rudolph C., Kaczmarek D, Gossler H, Drost S, Bykov V, Maas U, Schulz C. Flexible energy conversion and storage via high-temperature gas-phase reactions: The piston engine as a polygeneration reactor. Renewable and Sustainable Energy Reviews. 2020:133;110264. https://doi.org/10.1016/j.rser.2020.110264

[4] Hernández S, Farkhondehfal MA, Sastre F, Makkee M, Saracco G, Russo N. Syngas production from electrochemical reduction of CO_2: current status and prospective implementation. Green Chem. 2017:19;2326. https://doi.org/10.1039/C7GC00398F
[5] Heufer KA, Olivier H. Determination of ignition delay times of different hydrocarbons in a new high-pressure shock tube. Shock Waves. 2010:20;307–316. https://doi.org/10.1007/s00193-010-0262-2
[6] Curran HJ, Dunphy MP, Simmie JM, Westbrook CK, Pitz WJ. Shock tube ignition of ethanol, isobutene and MTBE: Experiments and modeling Proc. Symp. Combust. 1992:24;769−776. https://doi.org/10.1016/S0082-0784(06)80094-9
[7] Noorani EK, Akih-Kumgeh B, Bergthorson JM. Comparative High Temperature Shock Tube Ignition of C1−C4 Primary Alcohols. Energy Fuels 2010:24;5834-5843. https://doi.org/10.1021/ef1009692
[8] Cancino LR, Fikri M, Oliveira AAM, Schulz C. Measurement and chemical kinetics modeling of shock-induced ignition of ethanol–air mixtures. Energy Fuels 2010:24;2830–2840. https://doi.org/10.1021/ef100076w
[9] Lee C, Vranckx S, Heufer KA, Khomik SV, Uygun Y, Olivier H, Fernandez RX. On the chemical kinetics of ethanol oxidation: shock tube, rapid compression machine and detailed modeling study. Z. Phys. Chem. 2012:226;1–28.
[10] Mittal G, Burke SM, Davies VA, Parajuli B, Metcalfe WK, Curran HJ. Autoignition of ethanol in a rapid compression machine. Combust. Flame. 2014:161;1164–1171. https://doi.org/10.1016/j.combustflame.2013.11.005
[11] Li J, Kazakov A, Dryer FL. Ethanol pyrolysis experiments in a variable pressure flow reactor. Int. J. Chem. Kinet. 2001:33;859–867. https://doi.org/10.1002/kin.10009
[12] Li J, Kazakov A, Dryer FL. Experimental and numerical studies of ethanol decomposition reactions, J. Phys. Chem. A. 2004:108;7671–7680. https://doi.org/10.1021/jp0480302
[13] C.L. Barraza-Botet CL, S.W. Wagnon SW, M.S. Wooldridge MS. Combustion Chemistry of Ethanol: Ignition and Speciation Studies in a Rapid Compression Facility. J. Phys. Chem. A 2016: 120;7408−7418. https://doi.org/10.1021/acs.jpca.6b06725
[14] Haas FM, Chaos M, Dryer FL. Low and intermediate temperature oxidation of ethanol and ethanol–PRF blends: an experimental and modeling study. Combust. Flame. 2009:156;2346–2350. https://doi.org/10.1016/j.combustflame.2009.08.012
[15] Zhang Y, El-Merhubi H, Lefort B, Le Moyne L, Curran HJ, Kéromnès A. Probing the low-temperature chemistry of ethanol via the addition of dimethyl ether. Comb. Flame 2018:190:74-86. https://doi.org/10.1016/j.combustflame.2017.11.011
[16] Figueroa-Labastida M, Badra J, Elbaz AM, Farooq A. Shock tube studies of ethanol preignition. Comb. Flame 2018:198;176–185. https://doi.org/10.1016/j.combustflame.2018.09.011
[17] Aghsaee M, Nativel D, Bozkurt M, Fikri M, Chaumeix N, Schulz C. Experimental study of the kinetics of ethanol pyrolysis and oxidation behind reflected shock waves and in laminar flames. Proc. Combust. Inst. 2015:35;393–400. 10.1016/j.proci.2014.05.063
[18] Dunphy MP, Patterson PM, Simmie JM. High-temperature oxidation of ethanol. Part 2 - kinetic modelling, J. Chem. Soc., Faraday Trans. 87 (16) (1991) 2549–2559. https://doi.org/10.1039/FT9918702549
[19] Leplat N, Dagaut P, Togbé C, Vandooren J. Numerical and experimental study of ethanol combustion and oxidation in laminar premixed flames and in jet-stirred reactor. Combust Flame 2011:158;705-725. https://doi.org/10.1016/j.combustflame.2010.12.008
[20] Saxena P, Williams FA. Numerical and experimental studies of ethanol flames. Proc. Combust. Inst. 2007:31;1149–1156. DOI: 10.1016/j.proci.2006.08.097
[21 Marinov NM. A detailed chemical kinetic model for high temperature ethanol oxidation. Int. J. Chem. Kinet. 1999:31;183–220.
[22] Ranzi E, Frassoldati A, Grana R, Cuoci A, Faravelli T, Kelley AP, Law CK. Hierarchical and comparative kinetic modeling of laminar flame speeds of hydrocarbon and oxygenated fuels Prog. Energy Combust. Sci. 2012:38;468–501. https://doi.org/10.1016/j.pecs.2012.03.004
[23] Metcalfe WK, Burke SM, Ahmed SS, Curran HJ., A hierarchical and comparative kinetic modeling study of C1 −C2 hydrocarbon and oxygenated fuels. Int. J. Chem. Kinet. 2013:45;638–675. https://doi.org/10.1002/kin.20802
[24] Olm C, Varga T, Valkó É, Hartl S, Hasse C, Turányi T. Development of an ethanol combustion mechanism based on a hierarchical optimization approach. Int. J. Chem. Kinet. 2016:48;423–441. https://doi.org/10.1002/kin.20998
[25] Pinzón LT, Mathieu O, Mulvihill CR, Schoegl I, Petersen EL. Ethanol Pyrolysis Kinetics Using H2O Time History Measurements Behind Reflected Shock Waves. Proc. Comb. Inst. 2019:37;239-247. https://doi.org/10.1016/j.proci.2018.07.088
[26] Mathieu O, Pinzón LT, Atherley TM, Mulvihill CR, Schogel I, Petersen EL. Experimental study of ethanol oxidation behind reflected shock waves: Ignition delay time and H2O laser-absorption measurements. Comb. Flame 2019;208:313-326. https://doi.org/10.1016/j.combustflame.2019.07.005

[27] Choudhary R, Boddapati V, Clees S, Girard JJ, Peng Y, Shao J, Davidson DF, Hanson RK. Shock tube study of ethanol pyrolysis I: Multi-species time-history measurements. Comb. Flame 2021:233;111553. https://doi.org/10.1016/j.combustflame.2021.111553
[28] Choudhary R, Boddapati V, Clees S, Girard JJ, Peng Y, Shao J, Davidson DF, Hanson RK. Shock tube study of ethanol pyrolysis II: Rate constant measurements and modeling. Comb. Flame 2021:233;111554. https://doi.org/10.1016/j.combustflame.2021.111554
[29] Mulvihill C, Mathieu O, Petersen EL. H_2O time histories in the H_2-NO_2 system for validation of NOx hydrocarbon kinetics mechanisms. Int. J. Chem. Kinet. 2019;51:669-678. DOI: 10.1002/kin.21286
[30] Spearrin RM, Goldenstein CS, Jeffries JB, Hanson RK. Quantum cascade laser absorption sensor for carbon monoxide in high-pressure gases using wavelength modulation spectroscopy. Applied Optics, 2014;53:1938-1946. https://doi.org/10.1364/AO.53.001938
[31] Baigmohammadi M, Patel V, Nagaraja S, Ramalingam A, Martinez S, Panigrahy S, Mohamed A, Somers KP, Burke U, Heufer KA, Pekalski A, Curran H.J. Comprehensive experimental and simulation study of the ignition delay time characteristics of binary blended methane, ethane, and ethylene over a wide range of temperature, pressure, equivalence ratio, and dilution. Energy Fuels 2020;34:8808−8823. https://doi.org/10.1021/acs.energyfuels.9b04139
[32] Mathieu O, Mulvihill CR, Petersen EL. Assessment of modern detailed kinetics mechanisms to predict CO formation from methane combustion using shock-tube laser-absorption measurements. Fuel 2019:236;1164-1180. https://doi.org/10.1016/j.fuel.2018.09.029
[33] Alturaifi SA, Mathieu O, Mulvihill CR, Petersen EL. Using speciation measurements in Shock Tubes to help validating complex kinetics Mechanisms: Application to 2-methyl-2-butene oxidation. Comb. Flame 2021;225: 196-213. https://doi.org/10.1016/j.combustflame.2020.10.041
[34] Mulvihill CR, Keesee CL, Sikes T, Teixeira RS, Mathieu O, Petersen EL. Ignition delay times, laminar flame speeds, and species time-histories in the H_2S/CH_4 system at atmospheric pressure, Proc. Comb. Inst. 2021;37:735-742. https://doi.org/10.1016/j.proci.2018.06.034
[35] Mehl M, Pitz WJ, Westbrook CK, Curran HJ. Kinetic modeling of gasoline surrogate components and mixtures under engine conditions, Proceed. Combust. Inst. 2011:33;193-200. https://doi.org/10.1016/j.proci.2010.05.027
[36] Zhou C-W, Li Y, Burke U, Banyon C, Somers KP, Ding S, Khan S, Hargis JW, Sikes T, Mathieu O, Petersen EL, AlAbbad M, Farooq A, Pan Y, Zhang Y, Huang Z, Lopez J, Loparo Z, Vasu SS, Curran HJ. An Experimental and Chemical Kinetic Modeling Study of 1,3-Butadiene Combustion: Ignition delay time and laminar flame speed measurements. Comb. Flame 2018:197;423-438. https://doi.org/10.1016/j.combustflame.2018.08.006
[37] Dong S, Wagnon SW, Pratali Maffei L, Kukkadapu G, Nobili A, Mao Q, Pelucchi M, Cai L, Zhang K, Raju M, Chatterjee T, Pitz WJ, Faravelli T, Pitsch H, Senecal PK, Curran HJ. A new detailed kinetic model for surrogate fuels: C3MechV3.3. Applications in Energy and Combustion Science, 2022:9; 100043. https://doi.org/10.1016/j.jaecs.2021.100043
[38] Zhang H, Kaczmarek D, Rudolph C, Schmitt S, Gaiser N, Oßwaldd, P, Bierkandt T, Kasper T, Atakan B, Kohse-Höinghaus K. Dimethyl ether (DME) and dimethoxymethane (DMM) as reaction enhancers for methane: Combining flame experiments with model-assisted exploration of a polygeneration process. Comb. Flame 2022:237;111863. https://doi.org/10.1016/j.combustflame.2021.111863
[39] Pinzón LT, Mathieu O, Mulvihill CR, Schoegl I, Petersen EL. Ethanol Pyrolysis Kinetics Using H_2O Time History Measurements Behind Reflected Shock Waves. Proc. Comb. Inst. 2019:37;239-247. https://doi.org/10.1016/j.proci.2018.07.088
[40] Chemkin theory manual available at: https://personal.ems.psu.edu/~radovic/ChemKin_Theory_PaSR.pdf
[41] Senosiain JP, Klippenstein SJ, Miller JA. Pathways and rate coefficients for the decomposition of vinoxy and acetyl radicals. J. Phys. Chem. A 2006:110;5772-5781. https://doi.org/10.1021/jp054934r
[42] Faravelli T, Goldaniga A, Zappella L, Ranzi E, Dagaut P, Cathonnet M. An experimental and kinetic modeling study of propyne and allene oxidation. Proc. Combust. Inst. 2000:28;2601-2608. https://doi.org/10.1016/S0082-0784(00)80678-5